International Journal of Engineering Science and Advanced Technology (IJESAT)
Vol 26 Issue 11, November 2026
Received: 25-09-2026 Accepted: 29-10-2026 Published: 04-11-2026

Performance and Evaluation of Vortex Tube

Halavath Shankar[1], Bitragunta Naveen[2]
[12]*Asistant Professor, Department of Mechanical Engineering, Sri Chaitanya Institute of Technology and Research, Khammam, Telangana, India.*

Corresponding mail: halavath.shankar85@gmail.com

ABSTRACT

The vortex tube, or Ranque–Hilsch vortex tube, is a simple device with no moving parts that separates a stream of compressed gas into a cold and a hot stream. Its compactness, reliability and absence of refrigerants make it attractive for spot cooling, process cooling, cabinet cooling and gas conditioning, but its low efficiency has limited wider use. This paper evaluates the performance of a counter-flow vortex tube using a MATLAB-based thermodynamic parametric model that couples a choked-nozzle mass-flow relation, an energy balance between the two exit streams and empirical dependences of the temperature separation on inlet pressure, cold mass fraction, length-to-diameter ratio (L/D) and nozzle number. Inlet pressures of 2–6 bar (gauge) and cold mass fractions of 0.1–0.9 were considered with air supplied at 293 K. The cold-end temperature drop peaked near a cold fraction of 0.3 and rose from 25.0 K at 2 bar to 48.3 K at 6 bar; at 5 bar the maximum was 43.3 K, giving a cold-exit temperature of about 250 K. The hot-end temperature rise increased monotonically with cold fraction, reaching 50.4 K at 0.8. The cooling capacity peaked at a cold fraction of 0.5, rising from 34 W at 2 bar to 154 W at 6 bar, while the cooling coefficient of performance remained low at 0.11–0.12 and almost independent of pressure. An L/D near 20 and four or more nozzles gave the best separation. The results give practical guidance for selecting the operating point of a vortex tube according to whether maximum temperature drop or maximum cooling capacity is required.

Keywords: Vortex Tube, Ranque–Hilsch Effect, Cold Mass Fraction, Temperature Separation, Cooling Capacity, Coefficient of Performance, Compressed Air, MATLAB Simulation

I. INTRODUCTION

The vortex tube is a device that, with no moving parts, converts a stream of compressed gas at room temperature into two streams, one colder and one hotter than the supply. It was discovered by Ranque in the early 1930s [1] and developed into a practical device by Hilsch in the following decade [2], and it has therefore come to be known as the Ranque–Hilsch vortex tube. Because it requires only a source of compressed air, has no refrigerant, needs almost no maintenance, and is small, light and inexpensive, it is widely used for spot cooling of machining operations, cooling of electronic and electrical cabinets, cooling of gauges and sensors, hazardous-area cooling where electrical refrigeration is not allowed, and for gas drying and separation in laboratories [3], [4].

In its commonly used counter-flow form the compressed gas enters the tube tangentially through one or more nozzles and forms a rapidly rotating primary vortex that moves towards the hot end. A control valve at the hot end allows part of the gas to leave, while the remainder is reflected back along the axis as a secondary vortex that leaves through a central orifice at the cold end. The cold stream is colder than the supply and the hot stream is hotter, and the proportion of the gas leaving as the cold stream is called the cold mass fraction. The exact mechanism of energy separation has been discussed for decades, with explanations based on adiabatic expansion and compression, radial work transfer by the shear between the vortices, acoustic streaming and turbulent heat transfer; no single theory is universally accepted [3], [4].

Despite its simplicity, the vortex tube is much less efficient than a vapour-compression refrigerator, and its performance depends on a number of interacting variables: inlet pressure, nozzle configuration, cold fraction, tube length and diameter, cold orifice size and the working gas. A designer or user needs to know how the temperature drop, the cooling capacity and the efficiency vary with these parameters in order to choose an operating point. The objectives of the present paper are: (i) to formulate a thermodynamic parametric model of a counter-flow vortex tube; (ii) to evaluate by MATLAB the cold and hot temperature differences, cooling capacity and coefficient of

International Journal of Engineering Science and Advanced Technology (IJESAT)
Vol 26 Issue 11, November 2026
Received: 25-09-2026 Accepted: 29-10-2026 Published: 04-11-2026

performance for pressures of 2–6 bar and cold fractions of 0.1–0.9; (iii) to examine the influence of tube length-to-diameter ratio and the number of nozzles; and (iv) to provide guidelines for selecting the operating condition.

II. LITERATURE REVIEW

The review of Eiamsa-ard and Promvonge summarised the experimental and numerical work on the Ranque–Hilsch effect and showed that the temperature separation depends strongly on the inlet pressure, cold fraction and geometry, with the maximum cold temperature drop commonly occurring at cold fractions of 0.2–0.35 and the maximum cooling capacity at around 0.6–0.7 [3]. Xue et al. reviewed the physical explanations for temperature separation and concluded that the shear and work transfer between the two vortices is the most plausible mechanism, supplemented by the effects of compressibility and turbulence [4].

Computational fluid dynamics (CFD) has been used extensively. Aljuwayhel et al. used a CFD model with a turbulence closure to study the internal flow and found that the temperature separation could be reproduced qualitatively, with the energy transfer being controlled by the shear between the vortices [5]. Skye et al. compared CFD predictions with data from a commercial vortex tube and reported good agreement for the cold-end temperature but a lower accuracy for the hot end [6]. Behera et al. used CFD and experiments to optimise the nozzle profile and number of nozzles and found that nozzle design strongly influences the separation [7], and Promvonge and Eiamsa-ard examined the effect of tube length and cold-orifice diameter on the thermal separation [8]. Most of these studies concentrate on a single geometry and a few operating conditions. The present work instead provides a compact parametric model, easy to reproduce in MATLAB, from which the trends over the whole operating map can be obtained quickly.

III. MATERIALS AND METHODOLOGY

A. Vortex tube and working principle

The vortex tube considered is a counter-flow tube (Fig. 1) with a tangential nozzle assembly near the cold end, a cold orifice at the nozzle end and a hot-end valve that controls the cold mass fraction. Air at 293 K and a gauge pressure of 2–6 bar is supplied. The parameters of the model are summarised in Table 1.

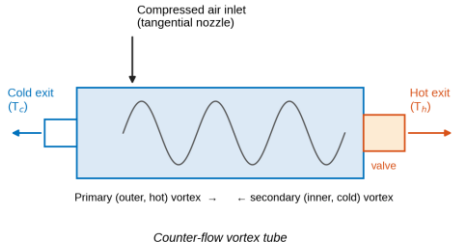


Fig. 1: Schematic of a counter-flow vortex tube showing the inlet, cold exit and hot exit

Table 1: Operating conditions and model parameters

Parameter	Value
Working fluid	Air (cp = 1005 J/kg·K, R = 287 J/kg·K)
Inlet temperature T_0	293 K
Inlet pressure P (gauge)	2, 3, 4, 5, 6 bar
Cold mass fraction μ_c	0.1–0.9
Tube L/D	10, 15, 20, 25, 30, 40
Number of nozzles n	1, 2, 4, 6
Mass-flow constant k	1.1×10^{-3} kg/s per bar (abs.)
$\Delta T_{c,max} = a P^b$	a = 16.5, b = 0.6 (P in bar)
Back pressure	Atmospheric (1 bar)

B. Methodology flow

The modelling procedure is shown in Fig. 2. The tube geometry and operating range are first defined; the nozzle mass flow, energy balance and temperature-separation relations are then used to compute the cold and hot temperatures; and the parametric sweeps in MATLAB generate the cold and hot temperature differences, the cooling capacity and the coefficient of performance. If the performance targets are not met, the pressure or geometry is changed.

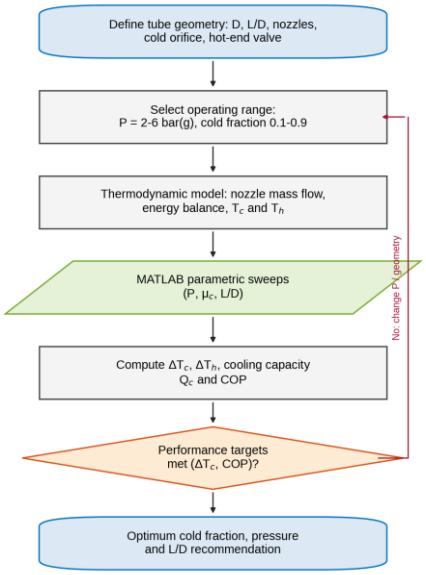


Fig. 2: Flow chart of the vortex tube performance evaluation procedure

International Journal of Engineering Science and Advanced Technology (IJESAT)
Vol 26 Issue 11, November 2026
Received: 25-09-2026 Accepted: 29-10-2026 Published: 04-11-2026

C. Mass flow and energy balance

The inlet nozzles are assumed to be choked at the pressures considered, so that the mass flow rate is proportional to the absolute supply pressure:

$$\dot{m} = k\,(P + 1) \quad (1)$$

where P is the gauge pressure in bar. With $k = 1.1 \times 10^{-3}$ kg/s per bar the flow rate is 3.3 g/s at 2 bar and 7.7 g/s at 6 bar. Applying the first law to the tube, which is assumed to be adiabatic with negligible change of kinetic energy and potential energy at the exits, gives

$$\mu_c\,\Delta T_c = (1 - \mu_c)\,\Delta T_h \quad (2)$$

where $\Delta T_c = T_0 - T_c$ is the cold-end temperature drop and $\Delta T_h = T_h - T_0$ is the hot-end temperature rise. This relation links the hot-end temperature to the cold one at any cold fraction and ensures energy conservation in the model.

D. Temperature-separation model

The cold-end temperature drop is represented by an asymmetric bell-shaped function of the cold fraction, with its maximum at $\mu_c = 0.3$ as seen in experiments [3], and a maximum value that depends on the inlet pressure:

$$\Delta T_c = \Delta T_{c,max}(P) \cdot \exp[-((\mu_c - 0.3)/s)^2], \quad \Delta T_{c,max} = a\,P^b \quad (3)$$

where $s = 0.22$ for $\mu_c < 0.3$ and $s = 0.45$ for $\mu_c \geq 0.3$, reflecting the faster decline of the separation at very low cold fractions and the slower decline at high cold fractions. The constants $a = 16.5$ and $b = 0.6$ were selected so that the maximum drop lies in the 25–50 K range commonly reported for compressed air at 2–6 bar. The L/D and nozzle-number dependences are represented by multiplicative factors applied to $\Delta T_{c,max}$:

$$f(L/D) = 1 - 0.5[(L/D - 20)/25]^2, \quad f(n) = 1 - 0.35\exp[-0.7(n - 1)] \quad (4)$$

E. Cooling capacity and coefficient of performance

The cooling capacity is the heat that the cold stream can absorb in being warmed back to the supply temperature, and the cooling coefficient of performance is defined relative to the reversible isothermal compression work of the air:

$$Q_c = \mu_c\,\dot{m}\,c_p\,\Delta T_c \quad (5)$$

$$COP = Q_c / W_{iso}, \quad W_{iso} = \dot{m}\,R\,T_0\,\ln(P_{abs}/P_{atm}) \quad (6)$$

The use of the isothermal work as the denominator is the usual way of expressing the work of compressed-air supply and gives a more favourable value than the actual compressor work, which is typically two or more times greater; the COP values presented are therefore upper bounds for real systems.

F. MATLAB implementation

The model was coded in MATLAB. Vectors of cold fraction (0.1–0.9 in steps of 0.005) and pressure (2–6 bar) were created, Eqs. (1)–(6) were evaluated by vectorised calculation, and the contour map of the cold temperature drop was produced with contourf. The calculation takes a fraction of a second and the parameters can be updated easily when experimental data become available, for instance by fitting a and b with lsqcurvefit.

IV. RESULTS AND DISCUSSION

A. Cold-end temperature drop

Fig. 3 shows the cold-end temperature drop versus the cold fraction. For every pressure the drop rises quickly to a maximum at $\mu_c = 0.3$ and then declines, being lowest at high cold fractions where a large proportion of the gas is forced out as cold gas with less energy removed per unit mass. The maximum drop increases with pressure from 25.0 K at 2 bar to 31.9, 37.9, 43.3 and 48.3 K at 3, 4, 5 and 6 bar, a total increase of 93 % for a threefold increase in gauge pressure, because a larger pressure ratio gives a stronger vortex and greater tangential velocity. At 5 bar and $\mu_c = 0.3$ the cold air leaves at about 250 K (–23 °C), which is enough for spot cooling and condensation-free drying.

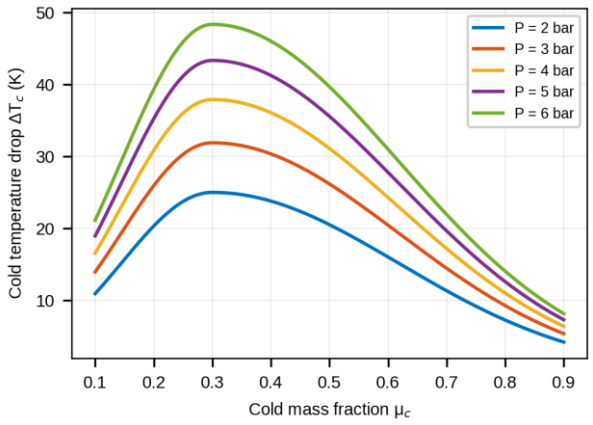


Fig. 3: Cold-end temperature drop versus cold mass fraction for inlet pressures of 2–6 bar

B. Hot-end temperature rise

The hot-end temperature rise given by the energy balance of Eq. (2) is plotted in Fig. 4. It increases continuously with the cold fraction, because the energy removed from the cold stream is

International Journal of Engineering Science and Advanced Technology (IJESAT)
Vol 26 Issue 11, November 2026
Received: 25-09-2026 Accepted: 29-10-2026 Published: 04-11-2026

shared among a smaller and smaller hot stream. At 5 bar the rise is 18.6 K at μ_c = 0.3, 35.6 K at 0.5 and 50.4 K at 0.8 (Table 2). If the objective is heating, or if a hot stream of high temperature is needed, the tube should therefore be operated at a high cold fraction, whereas for cooling it should be operated at a low-to-medium cold fraction.

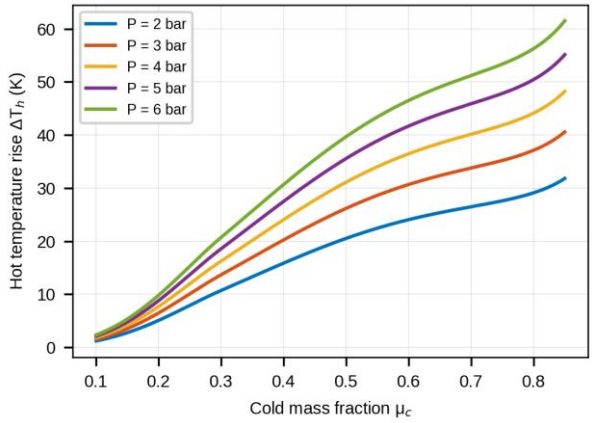


Fig. 4: Hot-end temperature rise versus cold mass fraction for inlet pressures of 2–6 bar

The absolute outlet temperatures at 5 bar are plotted in Fig. 5 for the 20 °C supply. The cold outlet is coldest, at about –23 °C, at μ_c = 0.3 and warms to about 7 °C at μ_c = 0.8, while the hot outlet rises from about 29 °C at 0.2 to about 70 °C at 0.8. The spread between the outlets, which is 50–60 K over most of the range, is the working temperature difference that a heat-exchange application can use.

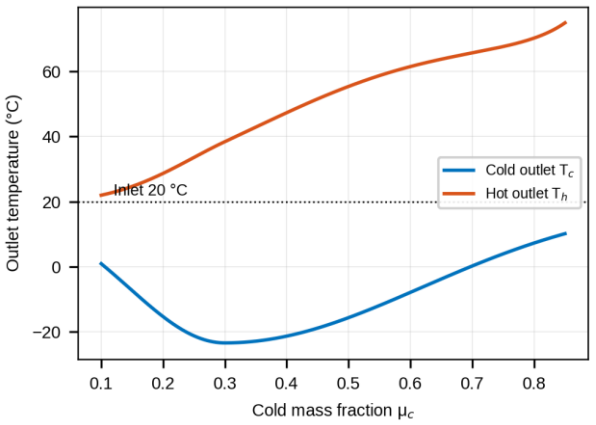


Fig. 5: Cold and hot outlet temperatures versus cold mass fraction at 5 bar (supply 20 °C)

Table 2: Performance at 5 bar (gauge) for different cold fractions

μ_c	ΔT_c (K)	ΔT_h (K)	Q_c (W)	COP
0.2	35.2	8.8	46.8	0.047
0.3	43.3	18.6	86.2	0.087
0.4	41.2	27.5	109.4	0.110
0.5	35.6	35.6	118.0	0.119
0.6	27.8	41.7	110.6	0.111
0.7	19.7	45.9	91.3	0.092
0.8	12.6	50.4	66.9	0.067

C. Cooling capacity and coefficient of performance

The cooling capacity (Fig. 6) is the product of the cold mass flow and the temperature drop, and therefore it peaks at a larger cold fraction than the temperature drop. At 5 bar the maximum cooling capacity is 118 W at μ_c = 0.5, with ΔT_c = 35.6 K. The COP follows the same trend and reaches a maximum of 0.119 at the same point; this is much less than the COP of a vapour-compression refrigerator, for which values of 2–4 are typical, and it explains why vortex tubes are used where simplicity, reliability and compactness matter more than efficiency. The COP at a cold fraction of 0.3, where the temperature drop is greatest, is 0.087, i.e. 27 % less than the maximum.

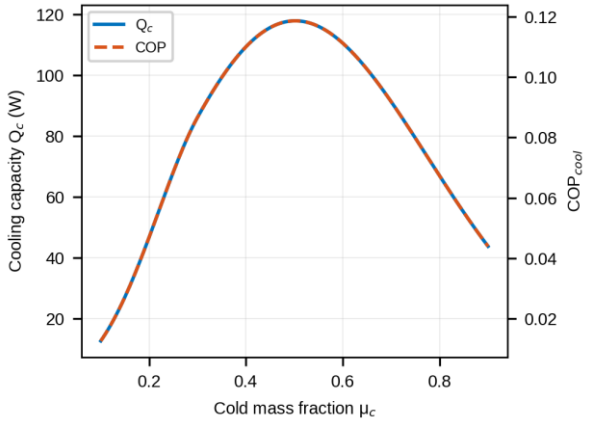


Fig. 6: Cooling capacity and COP versus cold mass fraction at 5 bar

D. Effect of inlet pressure

Table 3 gives the effect of pressure at the optimum cooling-capacity point (μ_c = 0.5). The mass flow increases linearly with pressure while the temperature drop increases more slowly, so the cooling capacity increases from 34.0 W at 2 bar to 153.5 W at 6 bar, a 4.5-fold increase, but the isothermal supply power increases from 305 W to 1260 W, a 4.1-fold increase. The COP therefore rises only slightly, from 0.112 to 0.122, and is almost independent of pressure. In practice this means that the choice of pressure is governed by the cooling load and the compressed-air supply available, and that raising the pressure is not an effective way of improving efficiency. A larger cooling load is better handled by several tubes at a moderate pressure than by raising the pressure in a single tube.

The combined influence of pressure and cold fraction on the cold temperature drop is summarised

International Journal of Engineering Science and Advanced Technology (IJESAT)
Vol 26 Issue 11, November 2026
Received: 25-09-2026 Accepted: 29-10-2026 Published: 04-11-2026

by the contour map of Fig. 7. The ridge of maximum separation lies along $\mu_c \approx 0.3$ at all pressures and moves to higher temperature drops as the pressure increases, so that the map can be used directly to read the operating pressure needed for a required temperature drop.

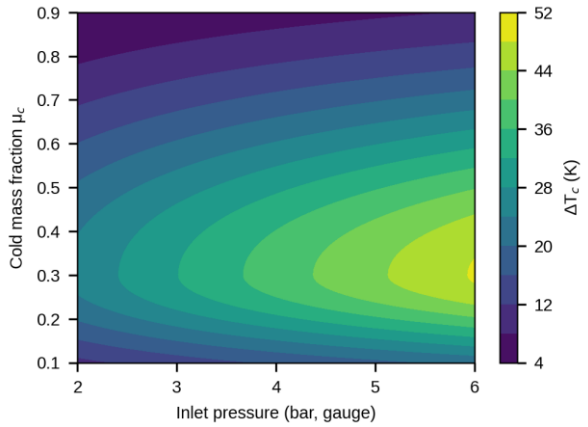


Fig. 7: Contour map of cold-end temperature drop as a function of pressure and cold fraction

Table 3: Effect of inlet pressure at $\mu_c = 0.5$

P (bar)	ṁ (g/s)	W_{iso} (W)	ΔT_c (K)	Q_c (W)	COP
2	3.3	305	20.5	34.0	0.112
3	4.4	513	26.2	57.9	0.113
4	5.5	744	31.1	86.0	0.116
5	6.6	994	35.6	118.0	0.119
6	7.7	1260	39.7	153.5	0.122

E. Effect of tube length-to-diameter ratio and nozzle number

The effect of L/D on the peak cold temperature drop at 5 bar is shown in Fig. 8. The maximum separation of 43.3 K occurs at L/D = 20, with slightly lower values of 42.5 K at 15 and 25 and 39.9 K at 10 and 30. At L/D = 40 the drop declines to 29.5 K, because the swirl decays and the secondary vortex is disrupted in a long tube, while in a short tube there is insufficient length for energy exchange between the vortices. L/D values of 15–30 are therefore recommended.

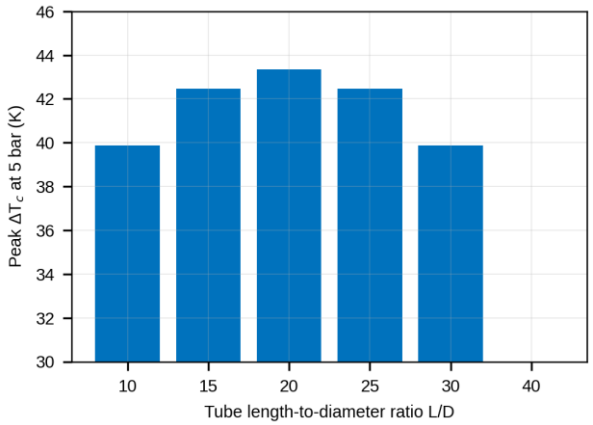


Fig. 8: Peak cold-end temperature drop at 5 bar for different L/D ratios

The number of nozzles has a strong effect on the separation (Table 4): the peak drop is 28.2 K with a single nozzle, 35.8 K with two, 41.5 K with four and 42.9 K with six at 5 bar. A single nozzle gives an asymmetric flow field, whereas several nozzles generate a more uniform swirl and reduce the losses in the entry region. The gain from four to six nozzles is only 1.4 K, so that four nozzles offer the best balance between performance and manufacturing complexity.

Table 4: Peak ΔT_c (K) at 5 bar for different L/D and nozzle numbers

L/D	10	15	20	25	30	40
ΔT_c (K)	39.9	42.5	43.3	42.5	39.9	29.5
Nozzles n	1	2	4	6		
ΔT_c (K)	28.2	35.8	41.5	42.9		

F. Second-law (exergy) analysis

The low COP can be understood from the second law. The specific flow exergy of a stream leaving at temperature T at ambient pressure, relative to the ambient state at T_0, is

$$ex = c_p[(T - T_0) - T_0 \ln(T/T_0)] \quad (7)$$

and the exergy efficiency is the ratio of the exergy of the two outlet streams, weighted by their mass fractions, to the isothermal compression work $R\,T_0 \ln(P_{abs}/P_{atm})$ that the compressed air represents. At 5 bar and $\mu_c = 0.5$ the cold stream (257.4 K) has an exergy of 2363 J/kg and the hot stream (328.6 K) 2009 J/kg, so the total outlet exergy is 2186 J/kg, compared with the 150.7 kJ/kg of the supplied compressed air. The exergy efficiency is thus only 1.45 % and is within 0.98–1.45 % for cold fractions of 0.3–0.7 (Fig. 9). The dominant loss, more than 98 % of the supplied exergy, is the throttling and irreversible mixing and dissipation in the nozzle and vortex, in which the pressure energy of the air is

International Journal of Engineering Science and Advanced Technology (IJESAT)
Vol 26 Issue 11, November 2026
Received: 25-09-2026 Accepted: 29-10-2026 Published: 04-11-2026

dissipated without doing useful work. This shows that large efficiency gains are unlikely from operating-point selection alone and that improvements must come from the design of the nozzle and vortex chamber, or from using the vortex tube where the compressed air is available at no extra cost, for example as a by-product of a pneumatic process.

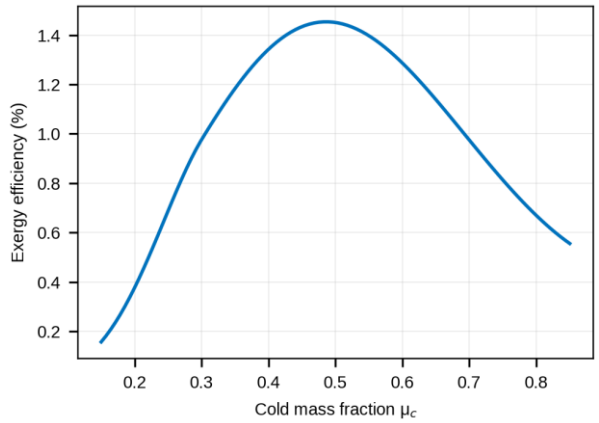


Fig. 9: Exergy efficiency of the vortex tube versus cold mass fraction at 5 bar

G. Worked example: spot cooling of a machining zone

Consider a 100 W heat load that must be removed from a machining zone using air at 20 °C. Table 2 shows that a single tube at 5 bar and μ_c = 0.5 delivers a cooling capacity of 118 W, with the cold air leaving at 257 K (–16 °C), so one tube is sufficient. The air consumption is 6.6 g/s, i.e. about 5.5 L/s (330 L/min) of free air at a density of 1.2 kg/m^3. Assuming a typical specific compressor power of about 6.5 kW per m^3/min of free air at 6–7 bar, the electrical input is about 2.1 kW, which is more than twice the isothermal work of 994 W, and the practical COP is only about 0.055. The vortex tube would therefore be a sensible choice if the cooling is needed intermittently, for example only during cutting, or if the simplicity and absence of coolant are the priority, but a refrigerated air chiller would be less costly to run for continuous duty. The comparison shows how the figures in Table 3 can be used for a quick sizing calculation.

H. Selection of the operating point

The results show that no single operating point is best. For the lowest possible cold temperature, for example in cooling a thermocouple or sample, the tube should be operated at the highest affordable pressure with a cold fraction of 0.2–0.35. For the largest cooling capacity, for example in cooling a machining zone or an electrical cabinet, the cold fraction should be 0.5–0.65, which gives about 35 % higher cooling capacity than at 0.3 (118 against 86 W at 5 bar) with a still useful 36 K temperature drop. For heating, or for use as a hot-air source, a cold fraction of 0.7–0.8 is required. A cold fraction of 0.4–0.6 therefore provides a good general-purpose compromise, with a COP of 0.11–0.12. These regions are summarised in Table 5.

Table 5: Recommended operating regions

Objective	Cold fraction	Typical result at 5 bar
Lowest cold temperature	0.2–0.35	$\Delta T_c \approx 43$ K
Maximum cooling capacity	0.5–0.65	$Q_c \approx 118$ W
Maximum COP	≈ 0.5	COP ≈ 0.12
Hot-air source	0.7–0.8	$\Delta T_h \approx 46$–50 K

I. Comparison with other cooling methods

Table 6 compares the vortex tube with a vapour-compression system and a thermoelectric cooler in qualitative terms. The vortex tube wins on simplicity, cost, absence of moving parts, response and suitability for hazardous or hot environments; it loses on efficiency and on the compressed-air consumption, which is the main running cost. Its use is therefore best restricted to intermittent or small-capacity spot-cooling duties, to locations where compressed air is already available, and to applications in which reliability and the absence of electrical components are a decisive advantage.

Table 6: Qualitative comparison with other cooling methods

Aspect	Vortex tube	Vapour compression	Thermoelectric
Moving parts	None	Compressor	None
Refrigerant	None	Required	None
Efficiency (COP)	Low (≈ 0.1)	High (2–4)	Low–moderate
Maintenance	Minimal	Regular	Low
Initial cost	Very low	High	Moderate
Hazardous areas	Suitable	Limited	Limited

J. Practical considerations

For a given installation, several practical measures help to improve the delivered performance. The compressed air should be dry and filtered because moisture and oil droplets reduce the separation and may freeze at the cold orifice. The supply line must be adequately sized, since pressure losses upstream of the nozzle directly reduce the effective inlet pressure. The cold stream should be ducted close to the point of use to avoid heat gain, and the hot stream should be silenced and vented away from the cooled region. Insulating the tube wall prevents heat exchange with the surroundings,

International Journal of Engineering Science and Advanced Technology (IJESAT)
Vol 26 Issue 11, November 2026
Received: 25-09-2026 Accepted: 29-10-2026 Published: 04-11-2026

which would invalidate the adiabatic assumption of Eq. (2) and lower the temperature difference, and a muffler on the hot exit reduces the noise level that is otherwise a nuisance in practice.

K. Sensitivity to the model constants

Because the constants of the model are assumed, it is important to know how the main results depend on them. Table 7 gives the cooling capacity and COP at 5 bar and $\mu_c = 0.5$ when each of k, a and b is changed in turn. The mass-flow constant k scales the cooling capacity in proportion but has no effect on the COP, since it cancels between the cooling capacity and the supply work; a 10 % error in k therefore only shifts the capacity from 106 to 130 W. The separation constants a and b influence both quantities in proportion to the cold temperature drop: a ±10 % change in a changes the COP by ±10 % (0.107–0.131), and a change of ±0.05 in the exponent b changes the values by about +8 % and –8 %. These ranges show that the qualitative conclusions, namely the position of the optimum cold fractions, the near independence of COP on pressure and the very low exergy efficiency, are robust, whereas the absolute values must be calibrated by experiment.

Table 7: Sensitivity of Q_c and COP at 5 bar, $\mu_c = 0.5$

Change	Q_c (W)	COP
Base case	118.0	0.119
k + 10 %	129.8	0.119
k – 10 %	106.2	0.119
a + 10 %	129.8	0.131
a – 10 %	106.2	0.107
b + 0.05	127.9	0.129
b – 0.05	108.9	0.109

L. Applications and design guidelines

The performance characteristics found above point to the applications in which vortex tubes are most effective. Spot cooling of cutting zones, welding seams and ultrasonic or laser processes needs a modest cooling capacity of the order of 100 W at a low temperature, which a single tube provides at an air consumption of a few litres per second. Cooling of control cabinets, sensors and cameras in dusty or explosive environments benefits from the absence of electrical parts and refrigerant. Laboratory uses include the chilling of small samples and of gas streams, and the vortex tube can also serve as a source of hot air for drying and de-icing. In each case the choice of operating point follows Table 5.

On the basis of the present analysis, the following design guidelines are proposed: (i) select the tube size from the required cooling load using Table 3 and Eq. (5), allowing a margin of 20–30 % for heat gains and pressure drops; (ii) use an L/D of 15–30 and at least four nozzles; (iii) set the hot-end valve to give a cold fraction of 0.5–0.65 for cooling-capacity duties, or 0.2–0.35 when the lowest temperature is needed; (iv) supply dry, filtered air at a regulated pressure of 5–6 bar, since a lower pressure reduces both the temperature drop and the capacity while a higher one barely improves the COP; and (v) where a continuous load is present, compare the compressed-air cost with that of a conventional refrigeration unit, since the vortex tube is seldom economical for continuous large-scale cooling.

V. LIMITATIONS AND FUTURE WORK

The results are produced by a parametric model, and their absolute values depend on the constants a, b, k and the shape factors, which were assigned from ranges reported in the literature. They should be calibrated against measurements on the actual tube. The model assumes steady, adiabatic operation with air as an ideal gas, and it neglects humidity, wall heat transfer, the cold-orifice diameter and the hot-end valve geometry. Future work includes an experimental set-up with calibrated thermocouples, flow meters and pressure gauges to validate the model, CFD analysis of the internal flow, the use of other gases such as nitrogen and CO_2, and the study of multi-stage and cascade arrangements and vortex-tube-assisted cooling of machining operations.

VI. CONCLUSION

A MATLAB-based parametric model of a counter-flow vortex tube was used to evaluate its performance. The cold-end temperature drop was a maximum at a cold fraction of 0.3 and rose from 25.0 K to 48.3 K when the pressure was increased from 2 to 6 bar, while the hot-end temperature rise increased steadily with cold fraction to 50.4 K at 0.8 (5 bar). The cooling capacity peaked at a cold fraction of 0.5, with 118 W at 5 bar and 153.5 W at 6 bar, with a COP of 0.11–0.12 that was almost independent of pressure. An L/D of about 20 and at least four nozzles gave the best separation. The

International Journal of Engineering Science and Advanced Technology (IJESAT)
Vol 26 Issue 11, November 2026
Received: 25-09-2026 Accepted: 29-10-2026 Published: 04-11-2026

vortex tube is thus best suited to compact, reliable, low-capacity spot-cooling duties, and its operating point should be selected according to whether the lowest temperature or the highest cooling capacity is required; experimental validation of the model is the next step.

Table 8: Nomenclature

Symbol	Meaning	Unit
μ_c	Cold mass fraction	–
ΔT_c, ΔT_h	Cold-end drop; hot-end rise	K
T_0, T_c, T_h	Inlet, cold and hot temperatures	K
P	Inlet gauge pressure	bar
$\dot{m}$	Inlet mass flow rate	kg/s
Q_c	Cooling capacity	W
W_{iso}	Isothermal compression work rate	W
COP	Cooling coefficient of performance	–
L/D	Tube length-to-diameter ratio	–
n	Number of nozzles	–

VII. REFERENCES

[1] Ranque, G. J. (1933). Expériences sur la détente giratoire avec productions simultanées d'un échappement d'air chaud et d'un échappement d'air froid. Journal de Physique et le Radium, 4(7), 112–114.

[2] Hilsch, R. (1947). The use of the expansion of gases in a centrifugal field as cooling process. Review of Scientific Instruments, 18(2), 108–113.

[3] Eiamsa-ard, S., & Promvonge, P. (2008). Review of Ranque–Hilsch effects in vortex tubes. Renewable and Sustainable Energy Reviews, 12(7), 1822–1842.

[4] Xue, Y., Arjomandi, M., & Kelso, R. (2010). A critical review of temperature separation in a vortex tube. Experimental Thermal and Fluid Science, 34(8), 1367–1374.

[5] Aljuwayhel, N. F., Nellis, G. F., & Klein, S. A. (2005). Parametric and internal study of the vortex tube using a CFD model. International Journal of Refrigeration, 28(3), 442–450.

[6] Skye, H. M., Nellis, G. F., & Klein, S. A. (2006). Comparison of CFD analysis to empirical data in a commercial vortex tube. International Journal of Refrigeration, 29(1), 71–80.

[7] Behera, U., Paul, P. J., Kasthurirengan, S., Karunanithi, R., Ram, S. N., Dinesh, K., & Jacob, S. (2005). CFD analysis and experimental investigations towards optimizing the parameters of Ranque–Hilsch vortex tube. International Journal of Heat and Mass Transfer, 48(10), 1961–1973.

[8] Promvonge, P., & Eiamsa-ard, S. (2005). Investigation on the vortex thermal separation in a vortex tube refrigerator. ScienceAsia, 31, 215–223.

[9] Çengel, Y. A., & Boles, M. A. Thermodynamics: An Engineering Approach. McGraw-Hill Education, New York.